Biosensors and Bioelectronics 68 (2015) 454–461

Contents lists available at ScienceDirect

Biosensors and Bioelectronics

journal homepage: www.elsevier.com/locate/bios

A novel pungency biosensor prepared with fixing taste-bud tissue of rats

Lixin Qiao [a], Lihua Jiao [a], Guangchang Pang [a,b,*], Junbo Xie [a,b,**]

[a] Biotechnology & Food Science College, Tianjin University of Commerce, Tianjin ,300134 China
[b] Tianjin Key Laboratory of Food Biotechnology, Tianjin ,300134 China

ARTICLE INFO

Article history:
Received 22 October 2014
Received in revised form
29 December 2014
Accepted 14 January 2015
Available online 15 January 2015

Keywords:
Taste biosensor
Capsaicin
Gingerol
Capsaicin receptor
Ligand

ABSTRACT

A novel taste biosensor based on ligand–receptor interaction was developed through fixing taste-bud tissues of SD rats to a glassy carbon electrode. Using the sodium alginate-starch gel as a fixing agent, taste-bud tissues of SD rats were fixed between two nuclear microporous membranes to make a sandwich-type sensing membrane. With the taste biosensor, the response current induced by capsaicin and gingerol stimulating the corresponding receptors was measured. The results showed that the lowest limit of detection of this biosensor to capsaicin was 1×10^{-13} mol/L and the change rate of response current was the highest at the concentration of 9×10^{-13} mol/L, indicating that the capsaicin receptor was saturated at this point. The lowest limit of detection of this biosensor to gingerol was 1×10^{-12} mol/L, and the gingerol receptor was saturated when the concentration of gingerol was 3×10^{-11} mol/L. It was demonstrated that the interaction curves of capsaicin and gingerol with their respective receptors exhibited high correlation (R^2: 0.9841 and 0.9904). The binding constant and dissociation constant of gingerol with its receptor were 1.564×10^{-11} and 1.815×10^{-11} respectively, which were all higher than those of capsaicin with its receptor (1.249×10^{-12} and 2.078×10^{-12}). This study, for the first time, made it possible to quantitatively determine the interaction of the taste receptor and pungent substances with a new biosensor, thus providing a simple approach for monitoring pungent substances and investigating the mechanism of ligand–receptor interaction.

1. Introduction

Taste, as an important physiological sense, can help specifically recognize and distinguish various taste substances. The taste-transduction process is a neurophysiological process, wherein some chemical information is converted to a second messenger molecule, thus causing the depolarization and Ca^{2+} release of taste cells. In other cases, the taste substance itself also act as cell signals (e.g., Na^+, K^+ and H^+) to induce action potential in taste-receptor cells. When the intercellular electrical signal reaches the threshold value, the nervous excitation can occur and be transmitted to the taste center in the brain so as to produce taste after multiple transductions (Yarmolinsky et al., 2009; Chandrashekar et al., 2006).

In the stripped taste mucosal epithelial tissue with taste buds, the taste receptor cells (TRCs) can retain their normal function well, and can be effectively activated by the taste substances in the invariant biological microenvironment. As a result, a new electrochemical biosensor with taste-bud tissues as the sensitive components can be developed through simulating the nerve-transduction mechanism of the taste (Fohlerova et al., 2007; El-Ali et al., 2006; Liu et al., 2006). Pungency is traditionally considered as a pain sense. Recently, the discovery of the pungent substance receptors, e.g., capsaicin receptor TRPV1 (Ramsey et al., 2006), has indicated that pungency is also a normal taste-transduction process. Although the qualitative and quantitative determination of the pungent substances has been conducted through various chemical methods (Ravishankar et al., 2000; Massa et al., 2006; Prescott and Julius, 2003), there have been few reported feasible methods to be used in the measurement of pungency up to now.

In most of the traditional studies of investigating the mechanism of ligand–receptor interaction, it is essential to purify the receptors first. However, when the receptors leave the cell membrane, the docking interactions of the membranes and the effects of certain intracellular cofactors do not exist any more. As a result, the real interaction mechanism of the receptor with its ligand cannot be accurately elucidated through the traditional method (Floriano et al., 2006; Walters and Hellekant, 2006; Omelyan and

* Corresponding author at: Biotechnology & Food Science College, Tianjin University of Commerce, Tianjin 300134, China. Fax: +86 2226675780.
** Corresponding author at: Biotechnology & Food Science College, Tianjin University of Commerce, Tianjin 300134, China.
E-mail addresses: pgc@tjcu.edu.cn (G. Pang), xjbo@tjcu.edu.cn (J. Xie).

http://dx.doi.org/10.1016/j.bios.2015.01.032
0956-5663/

Kovalenko, 2013).

In this study, a new pungency biosensor was developed with taste-bud tissues as the taste susceptor. Because it precisely simulated the ligand–receptor interaction environment in organisms, the biosensor could be used to elucidate the interaction mechanism of pungent substances with their receptors more accurately. Moreover, the binding constant and dissociation constant of ligand–receptor could be determined to investigate the kinetics with the biosensor (Nunez et al., 2012; Hughes et al., 2012), which could help to further explain the interaction mechanism of pungent substances with their receptors.

2. Experimental

2.1. Materials and apparatus

The CHI660E electrochemical workstation was purchased from Shanghai Chenhua Instruments, Inc (China). Nuclear microporous membrane (0.2 μm pore size, Circles, 25 mm) was obtained from Whatman Inc. (The United Kingdom).

Capsaicin and gingerol were obtained from Sigma (USA). Soluble starch was from Tianjin Yingda Sparseness & Nobel Reagent Chemical Factory (China). Sodium alginate was from Tianjin Guangfu Fine Chemical Institute (China). collagenase II and dispase II were obtained from Sigma (USA). All the other chemicals are of analytical grade. Deionized water was from a Millipore Milli-Q Water System (Millipore Inc.), and was used in all of the experiments.

2.2. Collection of taste-bud tissues

The solution of 1 mg/mL collagenase II and 3 mg/mL dispase II (prepared with calcium-free Tyrode's solution) was used to isolate the rat tongue epithelium, and preheated in an incubator at 37 °C for 15 min before experimentation. After the SD rats were sacrificed by decapitation, the tongues (from the tip to foliate papillae) were removed and washed with the solution for anatomy (137 mM NaCl, 10 mM HEPES, 1.5 mM NaH_2PO_4, 4.5 mM KH_2PO_4, 17 mM glucose and 22 mM sucrose; pH 7.2–7.4) to clean up the blood on the surface. 0.3–0.5 mL of the preheated solution (collagenase II and dispase II) was injected into the space between the tongue epithelium and its muscle layer. The tongues were then placed in the solution for anatomy and incubated at room temperature for 6–8 min. The tongue epithelium was gently stripped from the muscle layer, and immediately stored in the iced solution for anatomy.

2.3. Preparation of the taste-tissue sensor

The starch solution was prepared with dissolving proper amount of soluble starch in 1.0% glutaraldehyde (m/v). After being heated at 80 °C and stirred for 30 min, the solution was kept overnight at room temperature to make starch and glutaraldehyde fully crosslink. Then, the solution was mixed with 2.0% sodium alginate solution at a ratio of 1:1 to obtain sodium alginate-starch gel (Gao et al., 2009). After 10 μL of the gel solution was applied evenly over the two polycarbonate microporous membranes, the processed taste-bud epithelial tissue (10 mm^2) was placed on the center of one microporous membrane, which was then overlapped with the other microporous membrane.

The prepared sandwich-type membrane was immersed into 5.0% $CaCl_2$ solution for 10 s, thereby causing the gelatinization of sodium alginate solution to form a good fixed agent (Zactiti and Kieckbusch., 2009; Reiss et al., 1998; Bierhalz et al., 2014). In order to remove the remaining Cl^- and Ca^{2+}, the membrane was rinsed gently with 0.01 mol/L phosphate buffer (pH 7.0). Finally, the membrane was fixed to the surface of a glassy carbon electrode, and the taste-bud tissue should be coincided with the characterized electrode core. As shown in Fig. 1, the principle of the sensor was as follows: the binding of the pungency substance to the receptor would induce taste cell depolarization and Ca^{2+} release to generate action potentials, and the electrical signal was conducted to the central nervous system via specific nerves to produce the taste. This developed biosensor simulated this progress and conducted the electrical signal to the computer via the electrodes,

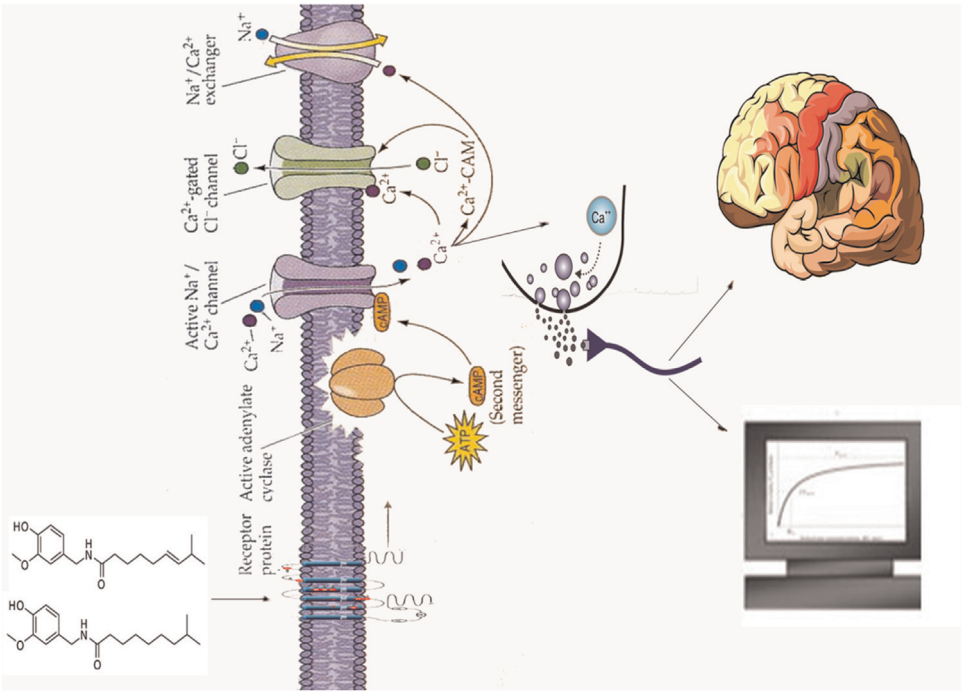

Fig. 1. Principle and scheme of the immobilized taste-bud tissue biosensor.

which displayed the interaction of the pungency ligand and its corresponding receptor.

2.4. Measurement of the pungent substance

The measurement was performed with a three electrode system: the glassy carbon electrode with fixed membrane for taste measurement as the working electrode, a Ag/AgCl electrode as the reference electrode, and a platinum wire electrode as the counter electrode. A solution mixed with 10 mL phosphate buffer (10 mM) and 1 mL NaOH aqueous solution (1 M) was used as the base solution. The response current, induced by different concentrations of capsaicin, gingerol and the mixture of the two substances, was determined through the current–time measurement method at a certain voltage. In this study, the change rate of response current was used as the detection index and calculated with Formula (1). When the response current difference between the determined solution and base solution was close to zero, the concentration of the determined substance was regarded as the lowest limit of detection.

$$\Delta I/\% = \frac{I_1 - I_2}{I_1} \times 100 \quad (1)$$

where I_1 and I_2 refer to the steady-state current values at the same time point before and after determining the pungency substance, respectively.

3. Results and discussion

3.1. Electrochemical characterization of pretreatment effect on the electrode

The activation treatment of the glassy carbon electrode with 1 mol/L sulfuric acid solution can induce the generation of negatively charged carboxyl, hydroxyl and other oxygen-containing groups, and cause the formation of porous structure on its surface, thereby increasing the effective surface area (Shi and Shiu, 2002; Nagaoka and Yoshino, 1986). The cyclic voltammogram of the activated glassy carbon electrode in 1 mol/L sulfuric acid solution (scan rate 50 mV/s, scan voltage range 0.6 to −0.1 V) was shown as Fig. 2A, which indicated that the peak potential difference was less than 80 mV, and the ratio of peak currents was close to 1. The alternating current impedance spectra (Fig. 2B) of the electrode (10^{-2}–10^{6} Hz) showed that the electron transferred onto the electrode surface merely via diffusion. From the cyclic voltammograms of the electrode at the scan rates of 25, 50, 75, 100, 125, 150, 200 and 250 mV/s (scan voltage range 0.6 to −0.1 V), as shown in Fig. 2C, there was a good linear relationship between all the redox peak currents and the square root of scan rates (Fig. 2D). For example, R^2 was 0.9989 at the scan rate of 50 mV/s. It indicated that the redox peak current of this glassy carbon electrode was only controlled by diffusion (The base solution was 1.0 mM $K_3Fe(CN)_6$ solution containing 0.2 M KNO_3).

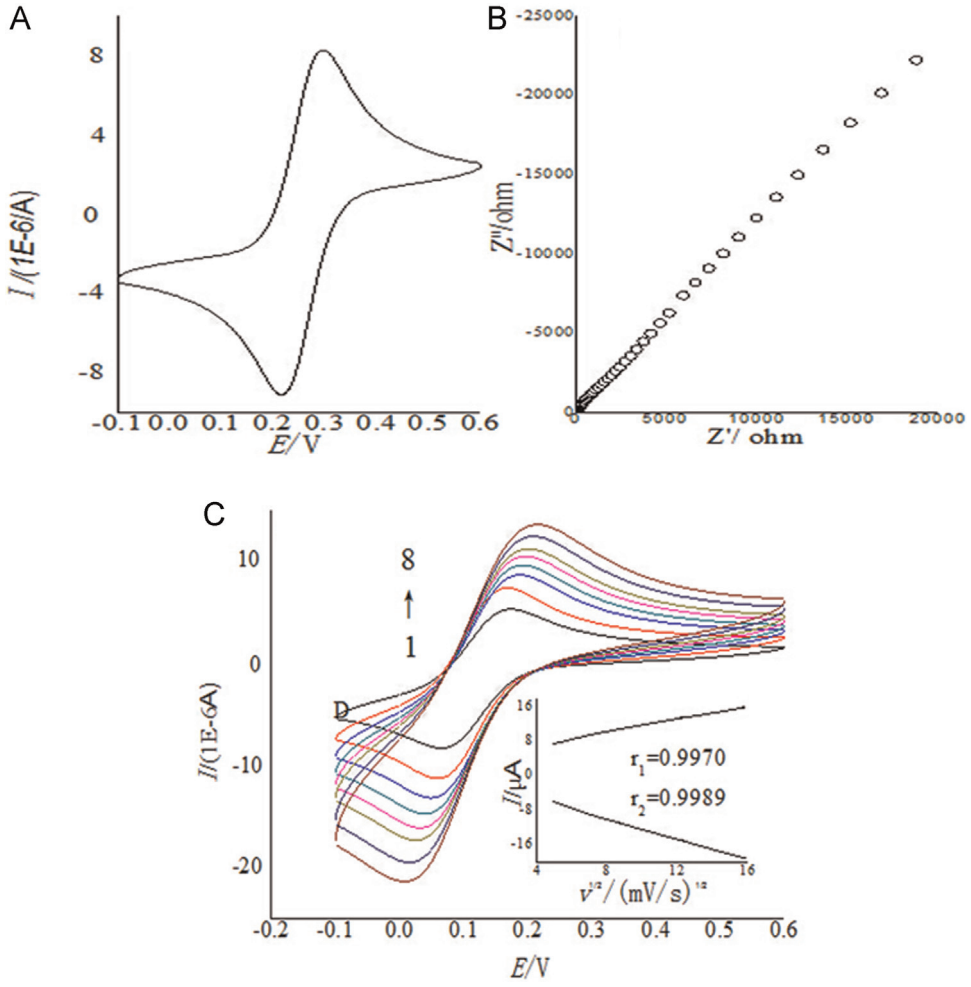

Fig. 2. (A) Cyclic voltammetry; (B) Alternating current impedance; (C) Cyclic voltammograms of bare glassy carbon electrode at the scan rate of 25, 50, 75, 100, 125, 150, 200, 250 mV/s (1→8); (D) Dependence of redox peak currents on the square root of scan rates.

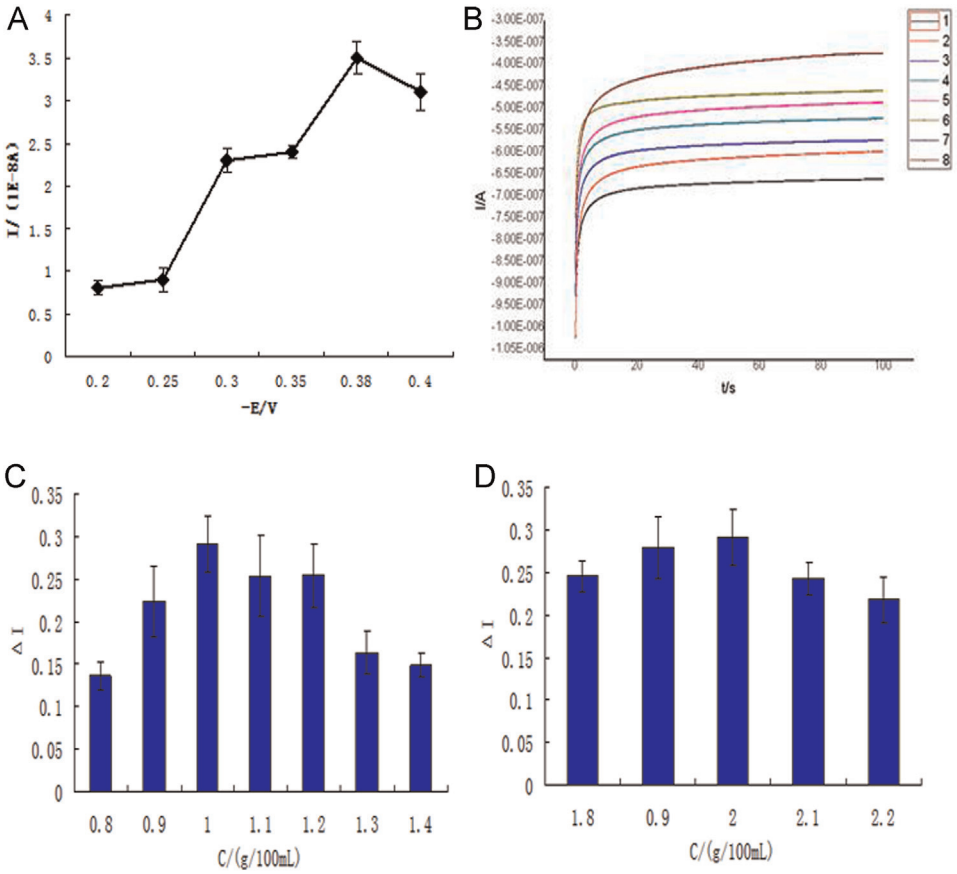

Fig. 3. (A) The effect of potentials on the electrochemical response of the biosensor; (B) the response current curve of the biosensor at different detection time; (C) the optimization of soluble starch concentration; and (D) the optimization of alginate concentration.

3.2. Potential optimization of the current–time measurement method and preparation of sodium alginate-starch gel

With the prepared biosensor, the potential optimization was investigated through the current–time method under different potentials (the base solution was 10 mM PBS solution at pH 7.4). The steady-state current difference before and after adding 10^{-5} mol/L capsaicin was adopted to evaluate the impact of different potentials on the electrochemical response of the sensor. The results (Fig. 3A) showed that the current had the maximum change rate at −0.38 V. Therefore, −0.38 V was selected as the constant voltage with which to investigate the response features of pungency biosensor to capsaicin and gingerol. In addition, the optimal time for detecting the response current was also investigated. Just as Fig. 3B, when the measurement of the pungent substances was performed, the response current achieved the steady station at 100 s. As a result, the detection time was set to be 100 s.

In this study, alginate-starch gel was used to fix the taste-bud epithelial tissue in the two polycarbonate microporous membranes. The concentrations of starch solution and sodium alginate in the preparation of alginate-starch gel would play a crucial role in the fixing effect (Gao et al., 2009). As a result, it is necessary to investigate their optimal concentrations. Soluble starch solutions were prepared at gradient concentrations of 0.8%, 0.9%, 1.0%, 1.1%, 1.2%, 1.3% and 1.4% (m/v) with 1% glutaraldehyde. The sodium alginate-starch gel was prepared with mixing the soluble starch solution and 2.0% sodium alginate at a ratio of 1:1. The pungency biosensor was assembled with the alginate-starch gel as the fixing agent (as described in Section 2.3), and the steady-state current of 10^{-5} mol/L capsaicin was measured by the time–current curve method. As in Fig. 3C, when the soluble starch solution concentration was 1.0%, the change rate of response current was the highest. As a result, the optimal concentration of the soluble starch solution was 1.0%. In the same way, the optimal sodium alginate concentration was investigated in the range of 1.8%, 1.9%, 2.0%, 2.1%, 2.2% (m/v). Just as in Fig. 3D, the result showed that the optimal concentration of the sodium alginate was 2.0%.

3.3. The interaction regularity of capsaicin and its receptor

The biosensor was assembled and utilized to measure capsaicin as described in Sections 2.3 and 2.4. The range of detectable capsaicin concentration was very wide, which made it difficult to describe the interaction regularity in the plot. As a result, the concentration of capsaicin was redefined as follows.

$$p\mathrm{Ca} = 14 + \mathrm{Log}\,(C) \tag{2}$$

where *p*Ca refers to the redefined concentration of capsaicin, and *C* refers to the predefined concentration of capsaicin.

From this formula, the minimum detectable concentration of capsaicin was 1×10^{-13} mol/L at *p*Ca = 1. The curve was drawn with *p*Ca as the *X* axis, and change rate of response current as the *Y* axis. As shown in Fig. 4A, the change rate of response current showed a good linear relationship with the capsaicin concentration in the range of 10^{-13}–10^{-12} mol/L. Consequently, the detectable concentration of capsaicin was further subdivided within 10^{-13}–10^{-12} mol/L, and the curve was shown as Fig. 4B. From the figure, the change rate was the highest when the determined concentration was 9×10^{-13} mol/L, indicating that the receptor was saturated by capsaicin at this concentration. The curve was further analyzed with hyperbola fitting. The fitted curve (Fig. 4C)

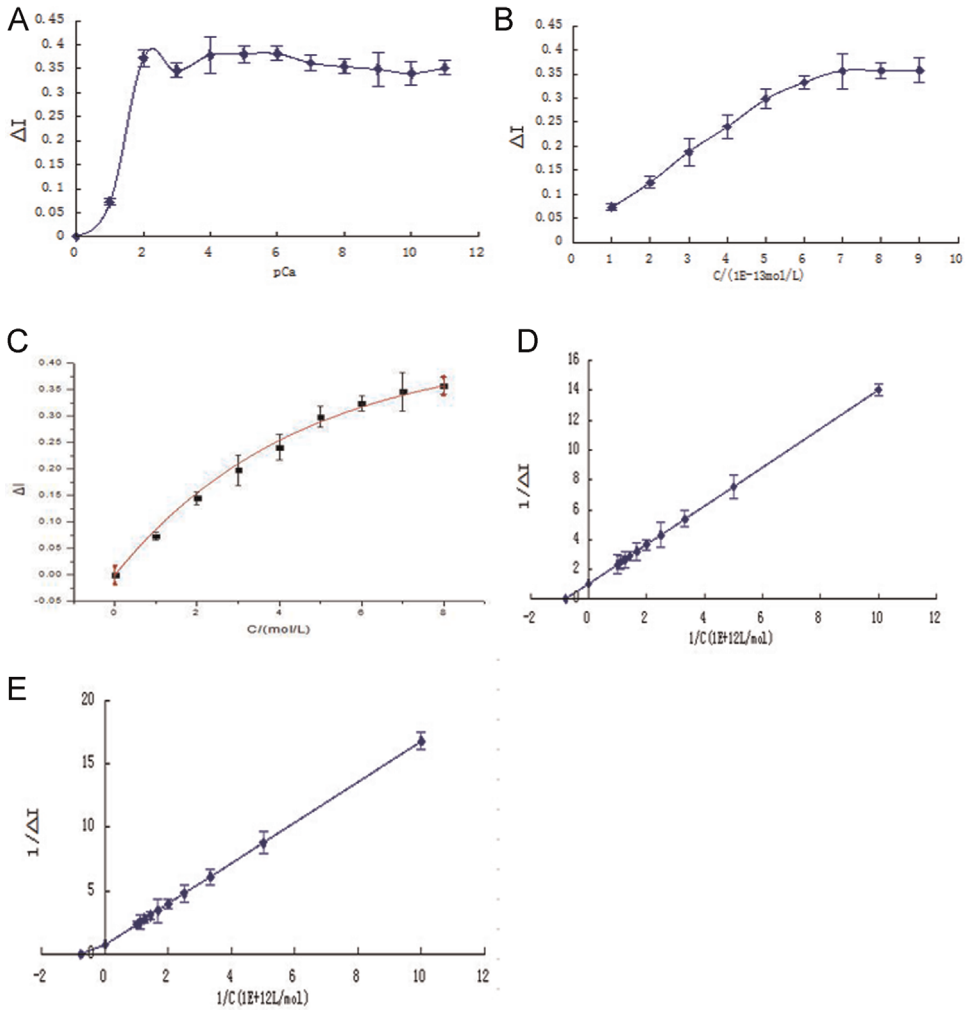

Fig. 4. (A) The detection range of capsaicin; (B) the interaction regularity regarding capsaicin (1×10^{-13}–9×10^{-13} mol/L) and its receptor; (C) the interaction regularity regarding capsaicin and its receptor (hyperbola fitted); (D) the measurement curve of capsaicin and its receptor binding constant; and (E) the measurement curve of capsaicin and its receptor dissociation constant.

showed a good linearity (R^2=0.9841), and the fitting equation was as follows:

$$\Delta I = 0.37565 - \frac{0.40268}{(1+(-1E12)C)^{1/-0.43551}}$$

Capsaicin solution with gradient concentrations was prepared from 1×10^{-13} mol/L to 9×10^{-13} mol/L, and the corresponding steady-state current was measured in ascending order of the capsaicin concentration. The change rate of response current at each concentration was calculated with the formula 1. As shown in Fig. 4 D, the curve was plotted with the reciprocal of capsaicin concentration as the *X* axis, and the reciprocal of change rate as the *Y* axis (double reciprocal plot). The curve showed a good linearity (R^2=0.9943), and the linear regression equation was as follows:

$$\frac{1}{\Delta I} = 1.3\times10^{-12}\frac{1}{C} + 1.0412\ (R^2 = 0.9943)$$

The binding constant K_a of capsaicin–receptor interaction was calculated to be 1.249×10^{-12} according to this equation.

Capsaicin solution with the same gradient concentrations was prepared, and the steady-state response current was measured. However, the measurement was performed in a decrement order (from high to low concentration). After the change rate of response current was calculated, the curve was plotted with the same method. As shown in Fig. 4E, the curve showed a good linearity (R^2=0.9901), and the linear regression equation was as follows:

$$\frac{1}{\Delta I} = 1.6\times10^{-12}\frac{1}{C} + 0.7701\ (R^2 = 0.9901)$$

The dissociation constant K_d of capsaicin–receptor interaction was calculated to be 2.078×10^{-12} according to this equation.

3.4. The interaction regularity of gingerol and its receptor

Just as capsaicin, the concentration of gingerol was redefined as follows:

$$p\,G = 13 + \mathrm{Log}\,(C) \qquad (3)$$

where *p*G refers to the redefined concentration of gingerol, *C* refers to the pre-defined concentration of gingerol.

From this formula, the minimum detectable concentration of capsaicin was 1×10^{-12} mol/L at *p*G=1. As shown in Fig. 5A, the curve was plotted with *p*G as the *X* axis and change rate of response current as the *Y* axis. It indicated that the change rate of response current had a good linear relationship with gingerol concentration in the range of 10^{-12}–10^{-11} mol/L. Hence, the detectable concentration of gingerol was further subdivided in the range of 10^{-12}–10^{-11} mol/L, and the curve was plotted as Fig. 5B. From the figure, the change rate was the highest when gingerol was 3×10^{-11} mol/L, indicating that the receptor was saturated at this concentration. The curve was further processed with

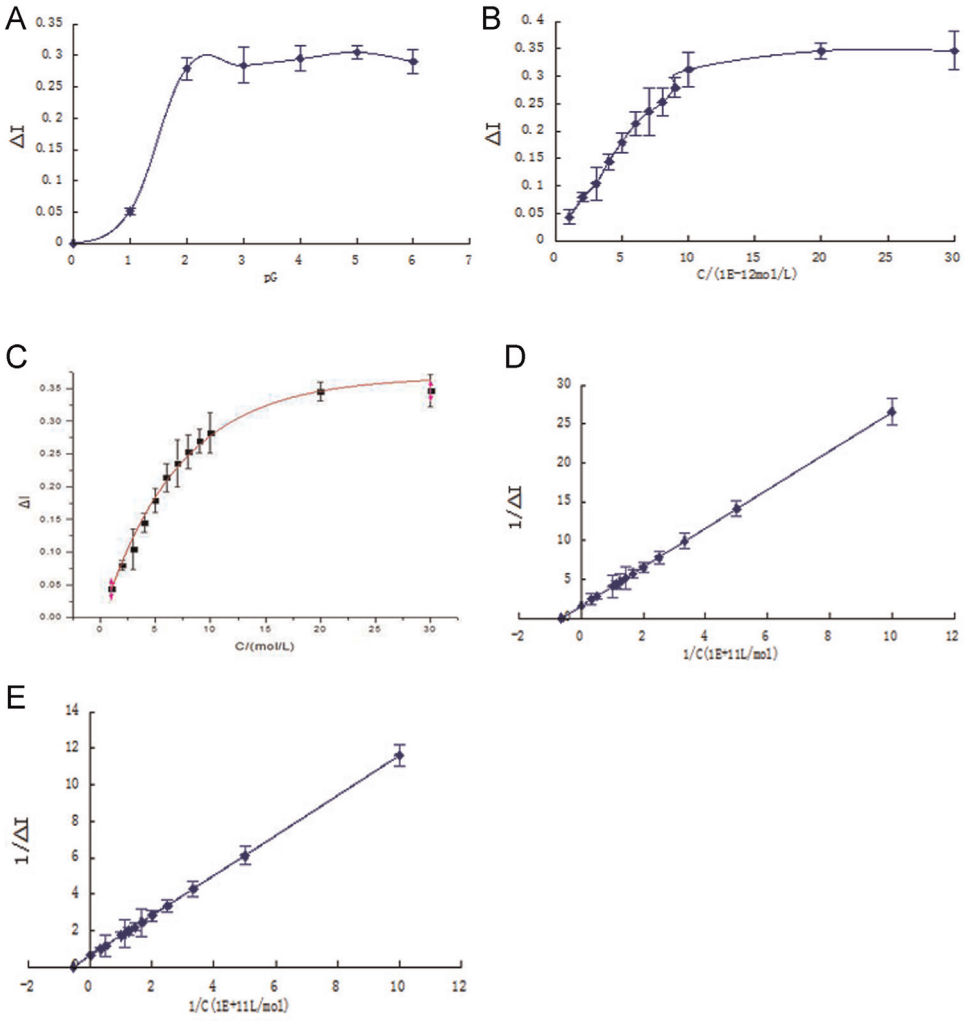

Fig. 5. (A) The interaction regularity regarding gingerol (1×10^{-12}–3×10^{-11} mol/L) and its receptor; (B) the detection range of gingerol; (C) the interaction regularity regarding gingerol and its receptor; (D) the measurement curve of gingerol and its receptor dissociation constant; (E) the measurement curve of gingerol and its receptor binding constant.

hyperbolic fitting, and the fitted curve (Fig. 5C) had good linearity (R^2=0.9904). The fitting equation was as follows:

$$\Delta I = 0.30457 - \frac{0.31821}{1 + (-3.33E10)C^{1/-0.22416}}$$

Gingerol solution was prepared with gradient concentrations of 1×10^{-13}–9×10^{-13} mol/L, and the corresponding steady-state current was measured in ascending order of the concentration. The change rate of response current at each concentration was calculated based on Formula (1). With the reciprocal of the concentration as the *X* axis and the reciprocal of change rate as the *Y* axis, the curve was plotted as Fig. 5D. The linear regression equation was as follows:

$$\frac{1}{\Delta I} = 2.5\times10^{-11}\frac{1}{C} + 1.5986\ (R^2 = 0.9965)$$

According to the equation, the binding constant K_a of gingerol-receptor interaction was calculated to be 1.564×10^{-11}.

Gingerol solution with the same concentration gradient was prepared, and the steady-state response current was measured in a decrement concentration order (from high to low). As shown in Fig. 5E, the curve (double reciprocal plot) was plotted with the above mentioned method. The linear regression equation was as follows:

$$\frac{1}{\Delta I} = 1.1\times10^{-11}\frac{1}{C} + 0.6062\ (R^2 = 0.9902)$$

According to the equation, the dissociation constant K_d of gingerol-receptor interaction was calculated to be 1.815×10^{-11}.

Compared with the binding constant (1.564×10^{-11}) and dissociation constant (1.815×10^{-11}) of gingerol, the constants of capsaicin (1.249×10^{-12} and 2.078×10^{-12} respectively) were smaller. It can be concluded that the affinity between capsaicin and its receptor was higher than that of gingerol and its receptor.

In this study, the biosensor, prepared with fixing rat taste-bud tissue, quantitatively measured the interaction mechanisms between capsaicin and gingerol with their taste receptors for the first time. The detection limit of capsaicin and gingerol were 1×10^{-13} mol/L and 1×10^{-12} mol/L, respectively. This suggested that rats were more sensitive to capsaicin (i.e., hotter for rats), which basically agreed with the human feeling. The interaction of the pungent substances with their receptors and the signal amplification can be described with Formula (4) (Supplementary information Fig. S1).

3.5. The interaction regularity regarding the mixture of capsaicin and gingerol with the receptor

The capsaicin and gingerol was mixed according to the concentrations in the Supplementary information Table S1 at a ratio of

Table 1
The reproducibility of the taste-tissue sensor.

Sensor number	Blank current (1×10^{-6} A)	Response current (1×10^{-6} A)	ΔI
01	-0.2707 ± 0.015	-0.1986 ± 0.012	26.635
02	-0.1343 ± 0.014	-0.0938 ± 0.007	30.134
03	-0.3348 ± 0.028	-0.2347 ± 0.017	29.898
04	-0.3890 ± 0.019	-0.2905 ± 0.024	25.321
05	-0.1112 ± 0.010	-0.0762 ± 0.006	31.475

1:1 (v/v), and the assembled taste-tissue sensor was used to measure the steady-state value of the response current, thus calculating the change rate of response current (Yarmolinsky et al., 2009). The results showed that, at low concentrations, the change rate of the solution of mixed capsaicin and gingerol was equal to the sum of their respective change rate. However, this additivity was not found at high concentrations.

It was demonstrated that the interaction of the two substances with their respective receptors was independent at the low concentration, but more complicated interactions occurred when the concentration exceeded a certain value. This also suggested that the receptors of capsaicin and gingerol were different. The complex interaction may be induced by the intracellular signal amplification, the cross-talk between signal pathways and the transmission process.

3.6. Stability and reproducibility of the biosensor

10 continuous measurements of the same concentration of capsaicin solution (10^{-5} mol/L) were performed with the biosensor. The calculated relative standard deviation (RSD) was 7.34%, which indicated that the biosensor had good stability. The biosensor was stored in PBS buffer at 4 °c, and was used to measure the same sample solution on consecutive 3 days. The result showed that the change rate of response current decreased only 5.7% after storage of 3 days. To investigate the reproducibility of the biosensor, 5 biosensors with different batch numbers were prepared and used to measure the same capsaicin solution. As shown in Table 1, the RSD of the change rate of response current (ΔI) was 9.03%, indicating that the sensor had good reproducibility.

Up to now, many various techniques have been used to detect the taste. The traditional electronic tongues mainly depend on physical–chemical absorption or the catalytic action of PVC film on the surface of the sensor to the specific substances. Because there is a gap in the process between this physical–chemical effect and the physical sensation that occurs in the biological taste system, the sensitivity of the traditional electronic tongue is obviously inferior to that of the biological taste system (Sghaier et al., 2009; Dias et al., 2014; Sehra et al., 2004). Additionally, the electronic tongue can only measure the substance, but cannot reflect the transduction process of taste via nerves. Although the electrode of unmodified noble-metal electrode sensor for measurement of the taste substance needs no modification, the differentiation among the chemical reactions occurring in different noble-metal electrodes is not clear (Winquist et al., 2000). The patch-clamp technique has been adopted to measure the molecular activity of a single or multiple ion channel(s). However, the puncture in the operation process may incur damage to the cells, which would change the cell characteristics and kill the cells within a few hours (Neher and Sakmann, 1976). Compared to the patch-clamp technique, the field-effect transistor (FET)-based biosensor can perform the long-term, real-time, non-destructive measurement of intercellular signal coupling and transduction. However, it cannot be guaranteed that the cells grow precisely in the fixation sites, as each measurement unit of FET is fixed (Fromherz et al., 1991). Zhang et al. have implemented an immobilization and positioning culture of a single cell on the surface of the sensor for measurement of taste substances. Because the taste process encompasses the combined action of all the taste cells as opposed to a selected cell, it cannot reflect the actual process of taste sensing. Moreover, it is difficult to ensure the cells grow on the electrode, which would decrease the efficiency of the method (Liu et al., 2013a, 2013b; Zhang et al., 2008).

Compared with the methods mentioned above, the newly developed biosensor can not only reflect the process of the rat taste-bud sensing, but can also simulate the taste nerve signal. Therefore, it is more accurate in describing the entire process of taste formation. The biosensor is based on the interaction of the ligand with its receptor. The interaction mechanism of the pungent substances with its receptors can be investigated efficiently, and the interaction kinetics parameters (such as binding constant and dissociation constant) can be assayed with the biosensor. This will help discover the physiological and nutritional function of the determined substances. It is well known that there are various receptors in the taste receptor cells, and even the same kind of receptor (such as TRPV1) can be activated by various ligands. As a result, this biosensor cannot measure and distinguish the mixed-taste substances.

4. Conclusion

In this study, a novel biosensor based on ligand–receptor interaction was developed through fixing taste-bud tissues and simulating the neurophysiological sensing process. The biosensor exhibited high sensitivity, wide linear range and low limit of detection in measuring capsaicin and gingerol. The binding and dissociation constants of the pungent substances with their receptors could be determined with this biosensor. This study provided a new idea for developing high sensitive taste biosensor and exploring the interaction mechanism of various sapid substances with their receptors. Moreover, the electrochemical mechanism mediating the transduction of the signal (i.e. capsaicin binding to its membrane receptor on the taste buds) into an electrical signal is still necessary to be investigated further.

Acknowledgements

The work was supported by the Open Research Fund for Key Laboratory of Dairy Science (Northeast Agricultural University), Ministry of Education, China (No. 2012KOLDSOF-02) and National Natural Science Foundation of China (No. 31371773).

Appendix A. Supplementary information

Supplementary data associated with this article can be found in the online version at http://dx.doi.org/10.1016/j.bios.2015.01.032.

References

Bierhalz, A.C.K., da Silva, M.A., Braga, M.E.M., Sousa, H.J.C., Kieckbusch, T.G., 2014. LWT-Food Sci. Technol. 57, 494–501.
Chandrashekar, J., Hoon, M.A., Ryba, N.J., Zuker, C.S., 2006. Nature 444, 288–294.
Dias, L.G., Fernandes, A., Veloso, A.C., Machado, A.A., Pereira, J.A., Peres, A.M., 2014. Food Chem. 160, 321–329.
El-Ali, J., Sorger, P.K., Jensen, K.F., 2006. Nature 442, 403–411.
Floriano, W.B., Hall, S., Vaidehi, N., Kim, U., Drayna, D., Goddard, W.A., 2006. J. Mol. Model. 12, 931–941.

Fromherz, P., Offenhausser, A., Vetter, T., Weis, J., 1991. Science 252, 1290–1293.
Fohlerova, Z., Skladal, P., Turanek, J., 2007. Biosens. Bioelectron. 22, 1896–1901.
Gao, Y.S., Pang, G.C., Li, J.P., 2009. Food Ferment. Ind. 5, 105–109.
Hughes, T.S., Chalmers, M.J., Novick, S., Kuruvilla, D.S., Chang, M.R., Kamenecka, T. M., Rance, M., Johnson, B.A., Burris, T.P., Griffin, P.R., Kojetin., D.J., 2012. Structure 20, 139–150.
Liu, Q., Cai, H., Xu., Y., Li, Y., Li, R., Wang, P., 2006. Biosens. Bioelectron. 22, 318–322.
Liu, Q.J., Zhang, D.M., Zhang, F.N., Zhao, Y., Hsia, K.J., Wang, P., 2013a. Sens. Actuators B: Chem. 176, 497–504.
Liu, Q.J., Zhang., F.N., Zhang, D.M., Hu, N., Wang, H., Hsia, K.J., Wang., P., 2013b. Biosens. Bioelectron. 40, 115–120.
Massa, F., Sibaev, A., Marsicano, G., Blaudzum, H., Storr, M., Lutz, B., 2006. J. Mol. Model. 84, 142–146.
Nagaoka, T., Yoshino, T., 1986. Anal. Chem. 58, 1037–1042.
Neher, E., Sakmann, B., 1976. Nature 260, 799–802.
Nunez, S., Venhorst, J., Kruse, C.G., 2012. Drug Discov. Today 17, 10–22.
Omelyan, I., Kovalenko, A., 2013. Mol. Simul. 39, 25–48.
Prescott, E.D., Julius, D.A., 2003. Science 300, 1284–1288.
Ramsey, I.S., Delling, M., Clapham, D.E., 2006. Annu. Rev. Physiol. 68, 619–647.
Ravishankar, G.A., Sarma, K.S., Venkatarama, L.V., Kadyan, A.K., 2000. Biotechnol. 76, 137–146.
Reiss, M., Heibges, A., Metzger, J., Hartmeier., W., 1998. Biosens. Bioelectron. 13, 1083–1090.
Sehra, G., Cole, M., Gardner, J.W., 2004. Sens. Actuators B: Chem. 103, 233–239.
Sghaier, K., Barhoumi, H., Maaref, A., Siadat, M., Jaffrezic-Renault, N., 2009. Sens. Lett. 7, 683–688.
Shi, K., Shiu, K.K., 2002. Anal. Chem. 74, 879–885.
Walters, D.E., Hellekant, G., 2006. J. Agric. Food Chem. 54, 10129–10133.
Winquist, F., Holmin, S., Krantz-Rulcker, C., Wide, P., Lundstrom, I., 2000. Anal. Chim. Acta 406, 147–157.
Yarmolinsky, D.A., Zuker, C.S., Ryba, N.J., 2009. Cell 139, 234–244.
Zactiti, E.M., Kieckbusch, T.G., 2009. Packag. Technol. Sci. 22, 349–358.
Zhang, W., Li, Y., Liu, Q.J., Xu, Y., Cai, H., Wang., P., 2008. Sens. Actuators B: Chem. 131, 24–28.